

# Clonogenic long-term survival assay of HCT 116 colorectal cancer cells after treatment with the synthesized diphenyl imidazoline derivatives

Youngshim Lee<sup>1</sup> · Dongsoo Koh<sup>2</sup> · Seunghyun Ahn<sup>1</sup> ·  
Young Han Lee<sup>3</sup> · Soon Young Shin<sup>3</sup> · Yoongho Lim<sup>1</sup>

Received: 8 February 2018 / Accepted: 21 February 2018 / Published online: 23 March 2018  
© The Korean Society for Applied Biological Chemistry 2018

**Abstract** Fourteen diphenyl imidazoline derivatives were designed, synthesized, and identified using NMR spectroscopy and high-resolution mass spectrometry. Their cytotoxicities in HCT 116 colorectal cancer cell lines were measured using a clonogenic long-term survival assay and the half-maximal cell growth inhibitory concentration (GI<sub>50</sub>) values were in the range 3.1–58.4 μM. As the anticancer effects of diphenyl imidazolines were reported to be caused by the inhibition of mouse double minute 2 homolog (MDM2), the inhibitory effects of the most potent derivative on MDM2 were assessed through Western blotting analysis. In silico docking experiments revealed the binding mode between this derivative and MDM2.

**Keywords** Diphenyl imidazolines · Colorectal cancer · MDM2 · Clonogenicity

## Introduction

During the last two decades, various diphenyl imidazolines have been synthesized and their biological activities have been evaluated. Antirheumatic, antidepressant, antiplasmodial, antitrypanosomal, and antimicrobial effects have been reported [1–6]. In addition, their potential as cardiovascular drugs, alpha 1-adrenoceptor antagonists, histone deacetylase-3 inhibitors, and spinal muscarinic M1 receptor activators have been tested [7–10] and their antitumor activity against HL60 cancer cells has also been reported [11].

Colorectal cancer refers to the cancer of the large intestine, colon, and the last part of the colon, the rectum. It is the third most common cancer in the USA, with more than 100,000 patients diagnosed in 2016, and it is the third-leading cause of cancer-related deaths [12]. The possible treatments include surgery, radiation therapy, and chemotherapy, but research into new chemotherapeutic agents is in progress. There are many methods to measure the anticancer effects of small compounds. One method is the measurement of their cytotoxicity in cancer cell lines [13–15]. Although the clonogenic long-term survival assay requires a time period of several days to obtain results for cytotoxic activities, it can distinguish the cytotoxicities between compounds containing a common skeleton [16]. To find diphenyl imidazolines that show cytotoxicity against colorectal cancer cell lines, 14 diphenyl-imidazoline derivatives were designed and synthesized. Their cytotoxicities in the HCT 116 colorectal cancer cell line were measured using a clonogenic long-term survival assay and their half-maximal cell growth inhibitory concentration (GI<sub>50</sub>) values were observed at the micromolar level. Recently, it was reported that the anticancer effects of

Youngshim Lee and Dongsoo Koh contributed equally to this work.

✉ Soon Young Shin  
shinsy@konkuk.ac.kr

✉ Yoongho Lim  
yoongho@konkuk.ac.kr; yoongholim@gmail.com

<sup>1</sup> Division of Bioscience and Biotechnology, BMIC, Konkuk University, Seoul 05029, Republic of Korea

<sup>2</sup> Department of Applied Chemistry, Dongduk Women's University, Seoul 02748, Republic of Korea

<sup>3</sup> Department of Biological Sciences, Konkuk University, Seoul 05029, Republic of Korea

diphenyl imidazolines were attributable to their inhibitory effects against mouse double minute 2 homolog (MDM2) [17–20]. Therefore, the most potent compound, (4R,5R)-2-(naphthalen-2-yl)-4,5-diphenyl-imidazoline, synthesized in this study was assessed for its inhibitory effect on MDM2 by Western blotting analysis. The binding mode between this compound and MDM2 was elucidated using in silico docking. The goal of this research was to study the structure–activity relationships (SARs) to suggest the structural features that contribute to the compound's strong cytotoxicity.

## Materials and methods

### Preparation of diphenyl imidazoline derivatives

(1R, 2R)-(+)-1,2-diphenylethylenediamine (DPEN, 11 mmol, 2.33 g) and *p*-methoxy benzaldehyde (10 mmol, 1.36 g) were dissolved in 100 mL *t*-BuOH. The mixture was stirred at room temperature for 30 min after which potassium carbonate (30 mmol, 4.14 g) and iodine (12.5 mmol, 3.15 g) were added to the mixture. The reaction mixture was stirred at 70 °C for 3 h. When the completion of the reaction was confirmed by thin layer chromatography, the reaction mixture was quenched with saturated Na<sub>2</sub>S<sub>2</sub>O<sub>5</sub> solution until the iodine color disappeared. The precipitate was filtered under vacuum and dried. The crude solid was recrystallized from ethanol. Yield 60%, m.p. 216–218 (white solid). The synthetic process is summarized in Scheme 1. Of 14 derivatives synthesized here, three derivatives **1**, **4**, and **9** have been reported previously.

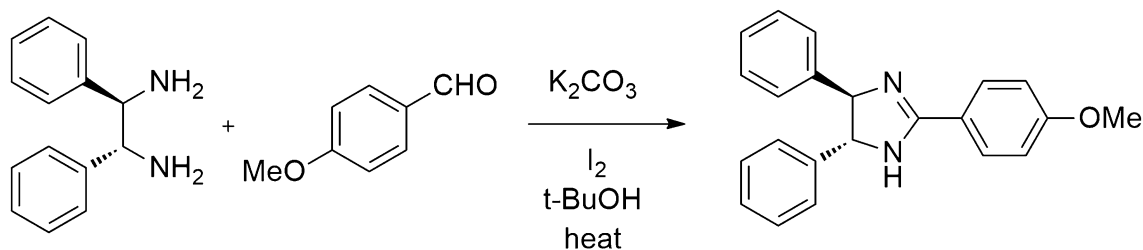
(4R,5R)-2-(4-methoxyphenyl)-4,5-diphenyl-imidazoline (**1**) [21] Ivory (18% yield); Mp = 216–218 °C; <sup>1</sup>H NMR (400 MHz, DMSO-*d*<sub>6</sub>) δ 7.95 (d, *J* = 8.6 Hz, 1H, H-2'), 7.43 (m, 2H, H-2/H-6), 7.36 (m, 2H, H-3/H-5), 7.24 (m, 1H, H-4), 7.03 (d, *J* = 8.6 Hz, 1H, H-3'), 4.84 (d, *J* = 8.3 Hz, 1H, Im-H-4), 4.63 (d, *J* = 8.3 Hz, 1H, Im-H-5), 3.82 (s, 3H, 4'-OCH<sub>3</sub>); <sup>13</sup>C NMR (100 MHz, DMSO-*d*<sub>6</sub>) δ 162.1 (Im-C-2), 161.2 (C-4'), 144.2 (C-1), 128.9 (C-2'/C-6'), 128.3 (C-3/C-5), 126.6 (C-4), 126.4 (C-2/C-6),

122.8 (C-1'), 113.6 (C-3'/C-5'), 79.3 (Im-C-4), 69.0 (Im-C-5), 55.2 (4'-OCH<sub>3</sub>); ν<sub>max</sub> (ATR) 3156 3024 2964 1614 cm<sup>-1</sup>; HRMS (m/z): Calcd. for C<sub>22</sub>H<sub>20</sub>N<sub>2</sub>O [M + H]<sup>+</sup>: 328.1627, Found. 328.1576.

(4R,5R)-2-(2,4,6-trimethoxyphenyl)-4,5-diphenyl-imidazoline (**2**) White (43% yield); Mp = 124–125 °C; <sup>1</sup>H NMR (400 MHz, CHCl<sub>3</sub>-*d*) δ 7.43 (d, *J* = 8.2 Hz, 2H, H-2/H-6), 7.34 (t, *J* = 7.1 Hz, 2H, H-3/H-5), 7.26 (m, 1H, H-4), 6.16 (s, 1H, H-3'), 4.84 (s, 2H, Im-H-4/Im-H-5), 3.86 (s, 6H, 2'-OCH<sub>3</sub>/6'-OCH<sub>3</sub>), 3.83 (s, 3H, 4'-OCH<sub>3</sub>); <sup>13</sup>C NMR (100 MHz, CHCl<sub>3</sub>-*d*) δ 162.0 (Im-C-2), 159.5 (C-4'), 159.2 (C-2'/C-6'), 143.9 (C-1), 128.1 (C-3/C-5), 126.7 (C-4), 126.2 (C-2/C-6), 102.4 (C-1'), 90.2 (C-3'/C-5'), 57.7 (Im-C-4/Im-C-5), 55.9 (2'-OCH<sub>3</sub>/6'-OCH<sub>3</sub>), 55.5 (4'-OCH<sub>3</sub>); ν<sub>max</sub>(ATR) 3152 3024 2901 1623 1588 cm<sup>-1</sup>; HRMS (m/z): Calcd. for C<sub>24</sub>H<sub>24</sub>N<sub>2</sub>O<sub>3</sub> [M + H]<sup>+</sup>: 388.1839, Found. 388.1787.

(4R,5R)-2-(4-nitrophenyl)-4,5-diphenyl-imidazoline (**3**) Pale yellow (26% yield); Mp = 200–202 °C; <sup>1</sup>H NMR (400 MHz, DMSO-*d*<sub>6</sub>) δ 8.35 (d, *J* = 8.9 Hz, 2H, H-3'/H-5'), 8.26 (d, *J* = 8.9 Hz, 2H, H-2'/H-6'), 7.36 (m, 1H, H-4), 7.33 (m, 2H, H-2/H-6), 7.26 (m, 2H, H-3/H-5), 4.96 (d, *J* = 8.4 Hz, 1H, Im-H-4), 4.74 (d, *J* = 8.4 Hz, 1H, Im-H-5); <sup>13</sup>C NMR (100 MHz, DMSO-*d*<sub>6</sub>) δ 160.8 (Im-C-2), 148.7 (C-4'), 143.6 (C-1), 136.0 (C-1'), 128.7 (C-2'/C-6'), 126.7 (C-4), 126.2 (C-2/C-6), 123.6 (C-3/C-5), 79.6 (Im-C-4), 69.3 (Im-C-5); ν<sub>max</sub>(ATR) 3124 3027 2930 1592 cm<sup>-1</sup>; HRMS (m/z): Calcd. for C<sub>21</sub>H<sub>17</sub>N<sub>3</sub>O<sub>2</sub> [M + H]<sup>+</sup>: 343.1385, Found. 343.1321.

(4R,5R)-2-(4-methylphenyl)-4,5-diphenyl-imidazoline (**4**) [22] Pale yellow (60% yield); Mp = 138–140 °C; <sup>1</sup>H NMR (400 Hz, DMSO-*d*<sub>6</sub>) δ 7.91 (d, *J* = 8.2 Hz, 2H, H-2'/H-6'), 7.37 (m, 2H, H-3/H-5), 7.29 (m, 2H, H-3'/H-5'), 7.28 (m, 2H, H-2/H-6), 7.27 (m, 1H, H-4), 4.76 (br s, 2H, Im-H-4/Im-H-5), 2.39 (s, 1H, 4-CH<sub>3</sub>); <sup>13</sup>C NMR (100 MHz, DMSO-*d*<sub>6</sub>) δ 162.2 (Im-C-2), 144.4 (C-1), 140.4 (C-4'), 129.0 (C-1'), 128.6 (C-3'/C-5'), 128.3 (C-3/C-5), 127.3 (C-2'/C-6'), 126.9 (C-4), 126.5 (C-2/C-6), 70.9 (Im-C-4/Im-C-5), 21.0 (4'-CH<sub>3</sub>); ν<sub>max</sub> (ATR) 3142 3025 2917 1624 1597 cm<sup>-1</sup>; HRMS (m/z): Calcd. for C<sub>22</sub>H<sub>20</sub>N<sub>2</sub> [M + H]<sup>+</sup>: 312.1706, Found. 312.1626.



**Scheme 1** The synthetic procedure for diphenyl imidazolines

(4*R*,5*R*)-2-(4-bromophenyl)-4,5-diphenyl-imidazoline (**5**) White (25% yield); Mp = 179–182 °C; <sup>1</sup>H NMR (400 MHz, DMSO-*d*<sub>6</sub>) δ 8.02 (d, *J* = 8.1 Hz, 1H, H-2'), 7.51 (m, 1H, H-3'), 7.36 (m, 2H, H-3'/H-5'), 7.32 (m, 1H, H-4), 7.28 (m, 2H, H-2/H-6), 4.78 (s, 2H, Im-H-4/Im-H-5); <sup>13</sup>C NMR (100 MHz, DMSO-*d*<sub>6</sub>) δ 162.3 (Im-C-2), 144.3 (C-1), 130.6 (C-1'), 130.2 (C-4'), 128.5 (C-3/C-5), 128.3 (C-4), 127.5 (C-3'/C-5'), 127.1 (C-2'/C-6'), 126.3 (C-2/C-6), 76.8 (Im-C-4), 70.7 (Im-C-5); *v*<sub>max</sub>(ATR) 3159 3027 2906 1610 cm<sup>-1</sup>; HRMS (m/z): Calcd. for C<sub>21</sub>H<sub>17</sub>BrN<sub>2</sub> [M + H]<sup>+</sup>: 376.0664, Found. 376.0575.

(4*R*,5*R*)-4,5-diphenyl-2-(thiophen-3-yl)-4,5-dihydro-1*H*-imidazole (**6**) Ivory (79% yield); Mp = 174–176 °C; <sup>1</sup>H NMR (400 MHz, DMSO-*d*<sub>6</sub>) δ 8.14 (dd, *J* = 1.3, 3.0 Hz, 1H, H-2'), 7.63 (dd, *J* = 3.0, 4.9 Hz, 1H, H-4'), 7.60 (dd, *J* = 1.3, 4.9 Hz, 1H, H-5'), 7.36 (m, 2H, H-3/H-5), 7.28 (m, 1H, H-4), 7.27 (m, 2H, H-2/H-6), 4.74 (s, 2H, Im-H-4/Im-H-5); <sup>13</sup>C NMR (100 MHz, DMSO-*d*<sub>6</sub>) δ 158.5 (Im-C-2), 144.1 (C-1), 132.8 (C-1'), 128.3 (C-3/C-5), 127.1 (C-4), 127.1 (C-5'), 126.9 (C-2'), 126.5 (C-4'), 126.2 (C-2/C-6), 79.1 (Im-C-4/Im-C-5); *v*<sub>max</sub>(ATR) 3159 3024 2893 1607 cm<sup>-1</sup>; HRMS (m/z): Calcd. for C<sub>19</sub>H<sub>16</sub>N<sub>2</sub>S [M + H]<sup>+</sup>: 304.1107, Found. 304.1034.

(4*R*,5*R*)-2-(4-chlorophenyl)-4,5-diphenyl-imidazoline (**7**) Ivory (81% yield); Mp = 168–172 °C; <sup>1</sup>H NMR (400 MHz, DMSO-*d*<sub>6</sub>) δ 8.03 (d, *J* = 8.5 Hz, 2H, H-2'/H-6), 7.56 (d, *J* = 8.5 Hz, 2H, H-3'/H-5'), 7.37 (m, 2H, H-3/H-5), 7.28 (m, 2H, H-2/H-6), 7.28 (m, 1H, H-4), 4.78 (s, 2H, Im-H-4/Im-H-5); <sup>13</sup>C NMR (100 MHz, DMSO-*d*<sub>6</sub>) δ 161.3 (Im-C-2), 144.0 (C-1), 135.3 (C-4'), 129.2 (C-2'/C-6'), 129.0 (C-1'), 128.5 (C-3/C-5), 128.4 (C-3'/C-5'), 127.1 (C-4), 126.4 (C-2/C-6), 74.3 (Im-C-4/Im-C-5); *v*<sub>max</sub>(ATR) 3152 3024 2917 1622 cm<sup>-1</sup>; HRMS (m/z): Calcd. for C<sub>21</sub>H<sub>17</sub>ClN<sub>2</sub> [M + H]<sup>+</sup>: 332.1157, Found. 332.1080.

(4*R*,5*R*)-2-(4-fluorophenyl)-4,5-diphenyl-imidazoline (**8**) Ivory (41% yield); Mp = 186–189 °C; <sup>1</sup>H NMR (400 MHz, DMSO-*d*<sub>6</sub>) δ 8.07 (d, *J* = 8.8 Hz, 2H, H-2'/H-6), 7.37 (m, 2H, H-3/H-5), 7.33 (d, *J* = 8.8 Hz, 2H, H-3'/H-5'), 7.32 (m, 2H, H-2/H-6), 7.25 (m, 1H, H-4), 4.88 (d, *J* = 7.2 Hz, 1H, Im-H-4), 4.67 (d, *J* = 7.2 Hz, 1H, Im-H-5); <sup>13</sup>C NMR (100 MHz, DMSO-*d*<sub>6</sub>) δ 164.7 (C-4'), 161.3 (Im-C-2), 144.0 (C-1), 129.8 (C-2'/C-6'), 128.4 (C-3/C-5), 126.7 (C-4), 126.7 (C-1'), 126.1 (C-2/C-6), 115.2 (C-3'/C-5'), 79.5 (Im-C-4), 69.3 (Im-C-5); *v*<sub>max</sub>(ATR) 3124 3027 2920 1618 cm<sup>-1</sup>; HRMS (m/z): Calcd. for C<sub>21</sub>H<sub>17</sub>FN<sub>2</sub> [M + H]<sup>+</sup>: 316.1463, Found. 316.1376.

(4*R*,5*R*)-2-(pyridine-2-yl)-4,5-diphenyl-imidazoline (**9**) [23] Yellow (62% yield); Mp = 122–125 °C; <sup>1</sup>H NMR (400 MHz, DMSO-*d*<sub>6</sub>) δ 8.69 (d, *J* = 4.8 Hz, 1H, H-3'), 8.18 (d, *J* = 7.9 Hz, 1H, H-6'), 7.95 (td, *J* = 1.7, 7.9 Hz, 1H, H-5'), 7.56 (dd, *J* = 4.7, 7.8 Hz, 1H, H-4'), 7.36 (m,

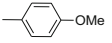
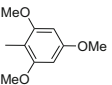
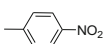
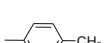

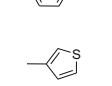
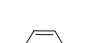

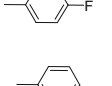
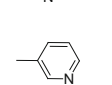
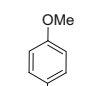
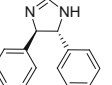
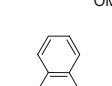
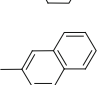
2H, H-3/H-5), 7.28 (m, 1H, H-4), 7.27 (m, 2H, H-2/H-6), 4.81 (br s, 2H, Im-H-4/Im-H-5); <sup>13</sup>C NMR (100 MHz, DMSO-*d*<sub>6</sub>) δ 162.2 (Im-C-2), 148.9 (C-3'), 148.5 (C-1'), 144.0 (C-1), 137.0 (C-5'), 128.5 (C-3/C-5), 127.1 (C-4), 126.4 (C-2/C-6), 125.5 (C-4'), 122.5 (C-6'), 69.0 (Im-C-4/Im-C-5); *v*<sub>max</sub>(ATR) 3281 3024 2911 1602 cm<sup>-1</sup>; HRMS (m/z): Calcd. for C<sub>20</sub>H<sub>17</sub>N<sub>3</sub> [M + H]<sup>+</sup>: 299.1518, Found. 299.1422.

(4*R*,5*R*)-2-(pyridine-3-yl)-4,5-diphenyl-imidazoline (**10**) Yellow (23% yield); Mp = 133–136 °C; <sup>1</sup>H NMR (400 MHz, Acetone-*d*<sub>6</sub>) δ 9.26 (dd, *J* = 0.7, 2.3 Hz, 1H, H-2'), 8.71 (dd, *J* = 1.7, 4.8 Hz, 1H, H-4'), 8.39 (dt, *J* = 1.9, 8.0 Hz, 1H, H-6'), 7.48 (ddd, *J* = 0.8, 4.8, 7.9 Hz, 1H, H-5'), 7.37 (m, 2H, H-3/H-5), 7.34 (m, 1H, H-4), 7.31 (m, 2H, H-2/H-6), 4.89 (s, 2H, Im-H-4/Im-H-5); <sup>13</sup>C NMR (100 MHz, Acetone-*d*<sub>6</sub>) δ 160.4 (Im-C-2), 151.0 (C-4'), 148.3 (C-2'), 143.7 (C-1), 134.3 (C-6'), 128.1 (C-3/C-5), 126.7 (C-4), 126.2 (C-2/C-6), 126.0 (C-1'), 122.8 (C-5'), 74.8 (Im-C-4/Im-C-5); *v*<sub>max</sub>(ATR) 3171 3030 2903 1599 cm<sup>-1</sup>; HRMS (m/z): Calcd. for C<sub>20</sub>H<sub>17</sub>N<sub>3</sub> [M + H]<sup>+</sup>: 299.1524, Found. 299.1422.

(4*R*,5*R*)-2,4,5-tris(4-methoxyphenyl)-4,5-dihydro-1*H*-imidazole (**11**) Cloudy yellow oil (27% yield); Mp = 150–154 °C; <sup>1</sup>H NMR (400 MHz, DMSO-*d*<sub>6</sub>) δ 7.92 (d, *J* = 8.8 Hz, 2H, H-2'/H-6'), 7.16 (d, *J* = 8.4 Hz, 2H, H-2/H-6), 7.02 (d, *J* = 8.8 Hz, 2H, H-3'/H-5'), 6.91 (d, *J* = 8.4 Hz, 2H, H-3/H-5), 4.63 (br s, 2H, Im-H-4/Im-H-5), 3.82 (s, 3H, 4'-OCH<sub>3</sub>), 3.74 (s, 3H, 4-OCH<sub>3</sub>); <sup>13</sup>C NMR (100 MHz, DMSO-*d*<sub>6</sub>) δ 161.5 (Im-C-2), 161.0 (C-4'), 158.6 (C-4), 136.3 (C-1), 129.0 (C-2'/C-6'), 127.5 (C-2/C-6), 122.8 (C-1'), 113.8 (C-3/C-5), 113.6 (C-3'/C-5'), 79.1 (Im-C-4/Im-C-5), 55.3 (4'-OCH<sub>3</sub>), 55.0 (4-OCH<sub>3</sub>); *v*<sub>max</sub>(ATR) 3161 3005 2928 2838 1610 cm<sup>-1</sup>; HRMS (m/z): Calcd. for C<sub>24</sub>H<sub>24</sub>N<sub>2</sub>O<sub>3</sub> [M + H]<sup>+</sup>: 388.1846, Found. 388.1787.

(4*R*,5*R*)-2-(naphthalene-1-yl)-4,5-diphenyl-imidazoline (**12**) Ivory (79% yield); Mp = 196–200 °C; <sup>1</sup>H NMR (400 MHz, DMSO-*d*<sub>6</sub>) δ 9.05 (dd, *J* = 1.6, 7.6 Hz, 1H, H-8'), 8.08 (d, *J* = 8.2 Hz, 1H, H-4'), 8.01 (d, *J* = 7.3 Hz, 1H, H-5'), 7.99 (dd, *J* = 1.2, 7.1 Hz, 1H, H-2'), 7.62 (m, 1H, H-3'), 7.60 (m, 1H, H-7'), 7.59 (m, 1H, H-6'), 7.40 (m, 2H, H-3/H-5), 7.38 (m, 2H, H-2/H-6), 7.32 (m, 1H, H-4), 4.87 (s, 2H, Im-H-4/Im-H-5); <sup>13</sup>C NMR (100 MHz, DMSO-*d*<sub>6</sub>) δ 163.2 (Im-C-2), 144.2 (C-1), 133.4 (C-1'), 130.7 (C-9'), 130.4 (C-4'), 128.6 (C-3/C-5), 128.3 (C-5'), 128.2 (C-10'), 127.7 (C-7'), 127.2 (C-2'), 127.2 (C-4), 126.5 (C-2/C-6), 126.3 (C-8'), 126.1 (C-6'), 125.0 (C-3'), 73.7 (Im-C-4/Im-C-5); *v*<sub>max</sub>(ATR) 3136 3027 2920 1563 cm<sup>-1</sup>; HRMS (m/z): Calcd. for C<sub>25</sub>H<sub>20</sub>N<sub>2</sub> [M + H]<sup>+</sup>: 348.1715, Found. 348.1626.

**Table 1** The names and structures of 14 diphenyl imidazolines and their half-maximal cell growth inhibitory concentrations (GI<sub>50</sub>)

Derivatives	R	Name	GI <sub>50</sub> /μM
1		(4 <i>R</i> ,5 <i>R</i> )-2-(4-methoxyphenyl)-4,5-diphenyl-imidazoline	17.9
2		(4 <i>R</i> ,5 <i>R</i> )-2-(2,4,6-trimethoxyphenyl)-4,5-diphenyl-imidazoline	5.3
3		(4 <i>R</i> ,5 <i>R</i> )-2-(4-nitrophenyl)-4,5-diphenyl-imidazoline	13.9
4		(4 <i>R</i> ,5 <i>R</i> )-2-(4-methylphenyl)-4,5-diphenyl-imidazoline	13.9
5		(4 <i>R</i> ,5 <i>R</i> )-2-(4-bromophenyl)-4,5-diphenyl-imidazoline	13.4
6		(4 <i>R</i> ,5 <i>R</i> )-4,5-diphenyl-2-(thiophen-3-yl)-4,5-dihydro-1 <i>H</i> -imidazole	29.3
7		(4 <i>R</i> ,5 <i>R</i> )-2-(4-chlorophenyl)-4,5-diphenyl-imidazoline	18.1
8		(4 <i>R</i> ,5 <i>R</i> )-2-(4-fluorophenyl)-4,5-diphenyl-imidazoline	23.0
9		(4 <i>R</i> ,5 <i>R</i> )-2-(pyridine-2-yl)-4,5-diphenyl-imidazoline	11.9
10		(4 <i>R</i> ,5 <i>R</i> )-2-(pyridine-3-yl)-4,5-diphenyl-imidazoline	58.4
11 <sup>a</sup>		(4 <i>R</i> ,5 <i>R</i> )-2,4,5-tris(4-methoxyphenyl)-4,5-dihydro-1 <i>H</i> -imidazole	14.3
12		(4 <i>R</i> ,5 <i>R</i> )-2-(naphthalene-1-yl)-4,5-diphenyl-imidazoline	8.1
13		(4 <i>R</i> ,5 <i>R</i> )-2-(naphthalene-2-yl)-4,5-diphenyl-imidazoline	3.1
14		(4 <i>R</i> ,5 <i>R</i> )-2-(4-methoxynaphthalene-1-yl)-4,5-diphenyl-imidazoline	5.1

<sup>a</sup>Does not show R, but does a complete structure

(4*R*,5*R*)-2-(naphthalene-2-yl)-4,5-diphenyl-imidazoline (**13**) Pearl white (9% yield); Mp = 70–76 °C; <sup>1</sup>H NMR (400 MHz, DMSO-*d*<sub>6</sub>) δ 8.57 (s, 1H, H-1'), 8.16 (dd, *J* = 1.6, 8.7 Hz, 1H, H-3'), 8.01 (d, *J* = 7.8 Hz, 1H, H-5'), 7.99 (m, 1H, H-3'), 7.61 (m, 1H, H-6'), 7.59 (m, 1H, H-7'), 7.37 (m, 2H, H-3/H-5), 7.34 (m, 2H, H-2/H-6), 7.31 (m, 1H, H-4), 4.84 (s, 2H, Im-H-4/Im-H-5); <sup>13</sup>C NMR (100 MHz, DMSO-*d*<sub>6</sub>) δ 162.4 (Im-C-2), 144.2 (C-1), 133.8 (C-10'), 132.4 (C-9'), 128.5 (C-3/C-5), 128.4 (C-8'), 127.8 (C-2'), 127.6 (C-4'), 127.3 (C-4), 127.3 (C-7'), 127.1 (C-1'), 126.7 (C-5'), 126.7 (C-6'), 126.5 (C-2/C-6), 124.8 (C-3'), 73.3 (Im-C-4/Im-C-5); ν<sub>max</sub>(ATR) 3142 3027 2895 1605 cm<sup>-1</sup>; HRMS (m/z): Calcd. for C<sub>25</sub>H<sub>20</sub>N<sub>2</sub> [M + H]<sup>+</sup>: 348.1716, Found. 348.1626.

(4*R*,5*R*)-2-(4-methoxynaphthalene-1-yl)-4,5-diphenyl-imidazoline (**14**) White (11% yield); Mp = 172–176 °C; <sup>1</sup>H NMR (400 MHz, DMSO-*d*<sub>6</sub>) δ 9.23 (dm, *J* = 8.2 Hz, 1H, H-8'), 8.26 (dm, *J* = 8.1 Hz, 1H, H-5'), 7.98 (d, *J* = 8.1 Hz, 1H, H-2'), 7.61 (ddd, *J* = 1.2, 7.1, 8.2 Hz, 1H, H-7'), 7.56 (ddd, *J* = 1.1, 7.1, 8.1 Hz, 1H, H-6'), 7.40 (m, 2H, H-3/H-5), 7.36 (m, 2H, H-2/H-6), 7.36 (m, 1H, H-4), 7.07 (d, *J* = 8.1 Hz, 1H, H-3'), 4.99 (d, *J* = 6.3 Hz, 1H, Im-H-4), 4.66 (d, *J* = 6.3 Hz, 1H, Im-H-5), 4.04 (s, 3H, 4'-OCH<sub>3</sub>); <sup>13</sup>C NMR (100 MHz, DMSO-*d*<sub>6</sub>) δ 163.2 (Im-C-2), 156.4 (C-4'), 144.3 (C-1), 131.9 (C-9'), 128.6 (C-2'), 128.4 (C-3/C-5), 127.1 (C-4), 126.7 (C-8'), 126.5 (C-2/C-6), 126.3 (C-7'), 125.5 (C-6'), 125.0 (C-10'), 121.6 (C-5'), 120.1 (C-1'), 103.5 (C-3'), 80.6 (Im-C-4), 68.5 (Im-C-5), 55.9 (4'-OCH<sub>3</sub>); ν<sub>max</sub>(ATR) 3161 3029 2938 1582 cm<sup>-1</sup>; HRMS (m/z): Calcd. for C<sub>26</sub>H<sub>22</sub>N<sub>2</sub>O [M + H]<sup>+</sup>: 378.1837, Found. 378.1732.

### Identification of diphenyl imidazoline derivatives

The structures and names of the diphenyl imidazolines synthesized in this work are listed in Table 1. The compounds were dissolved in deuterated dimethyl sulfoxide (DMSO-*d*<sub>6</sub>), chloroform (CHCl<sub>3</sub>-*d*), and acetone (CH<sub>3</sub>-COCH<sub>3</sub>-*d*<sub>6</sub>) for nuclear magnetic resonance (NMR) spectroscopy and adjusted to a concentration of approximately 50 mM. These solutions were transferred to 2.5-mm NMR tubes. All NMR spectra were collected using an Avance 400 spectrometer system (9.4 T; Bruker, Karlsruhe, Germany) at 25 °C. The NMR experimental conditions used are similar to those employed in a previous study [24]. To confirm the structures of the diphenyl-imidazoline derivatives, ultraperformance liquid chromatography-hybrid quadrupole-time-of-flight mass spectrometry was performed using a Waters Acquity UPLC system (Waters Corp., Milford, MA) with the help of Prof. Choong Hwan Lee at Konkuk University, Korea [25]. All high-resolution mass spectrometric (HRMS) data consisted of M + H ions.



Melting points and IR spectra were measured using a Mel-Temp II (LabX, Midland, ON, Canada) and an FT-IR 4200 spectrometer (JASCO, Easton, MD) equipped with an ATR (Attenuated Total Reflection, ATR PR0450-S), respectively [26]. The melting points and spectroscopic data for the 14 diphenyl imidazoline derivatives obtained from NMR spectroscopy, HRMS, and IR are summarized in the references and notes.

### Biological evaluation of diphenyl imidazoline derivatives

HCT 116 human colorectal cancer cells were used for the cytotoxicity tests of the diphenyl imidazoline derivatives. The long-term clonogenic survival data were collected in the absence or presence of different concentrations (0, 1, 5, 10, and 20  $\mu\text{M}$ ) of the 14 derivatives. The procedures adhered to previously reported methods [27]. The results were analyzed using densitometry (MultiGauge, Fujifilm, Japan), and the  $\text{GI}_{50}$  values were determined using SigmaPlot software (SYSTAT, Chicago, IL, USA) (Table 1) [28].

For the detection of MDM2 activity, the phosphorylation of the MDM2 protein at S166 was measured by immunoblotting analysis. HCT 116 cells were treated with 40  $\mu\text{M}$  derivative **13**, (4R,5R)-2-(naphthalene-2-yl)-4,5-diphenyl-imidazoline, for various time periods (0, 3, 6, 12,

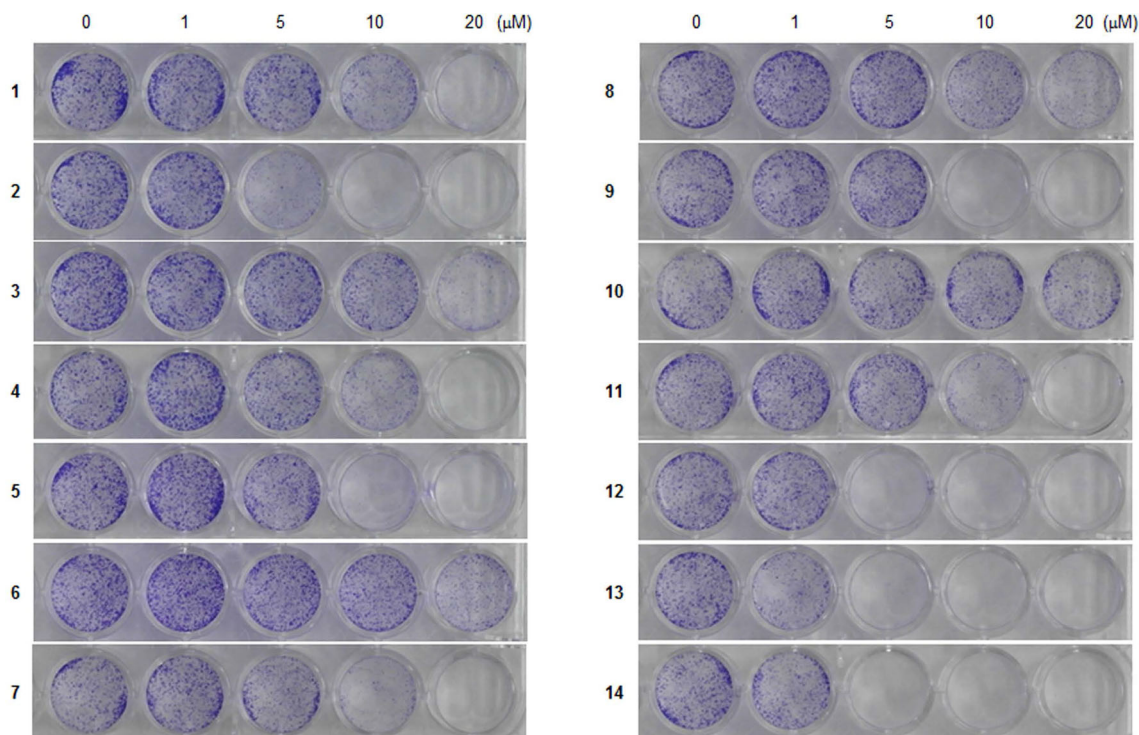
or 24 h) and then extracted with cell lysis buffer (25 mM Tris-HCl pH 7.5, 1% Triton X-100, 10% glycerol, 150 mM NaCl, 1 mM  $\text{Na}_3\text{VO}_4$ , and 10 mg/mL leupeptin). Protein extracts were electrophoresed on a 10% SDS-polyacrylamide gel, transferred to nitrocellulose membranes, and incubated with anti-phospho-MDM2 antibody (Cell Signaling Technology, Beverly, MA, USA). The glyceraldehyde phosphate dehydrogenase (GAPDH) antibody from Santa Cruz Biotechnology (Santa Cruz, CA, USA) was used as an internal control. The blots were developed using the enhanced chemiluminescence detection system (GE Healthcare, Piscataway, NJ, USA) [29].

### Statistical analysis

Statistical analyses were conducted using a one-way analysis of variance (ANOVA), followed by Kruskal–Wallis test, by using GraphPad InStat software (La Jolla, CA). All experiments were performed in triplicate [30].

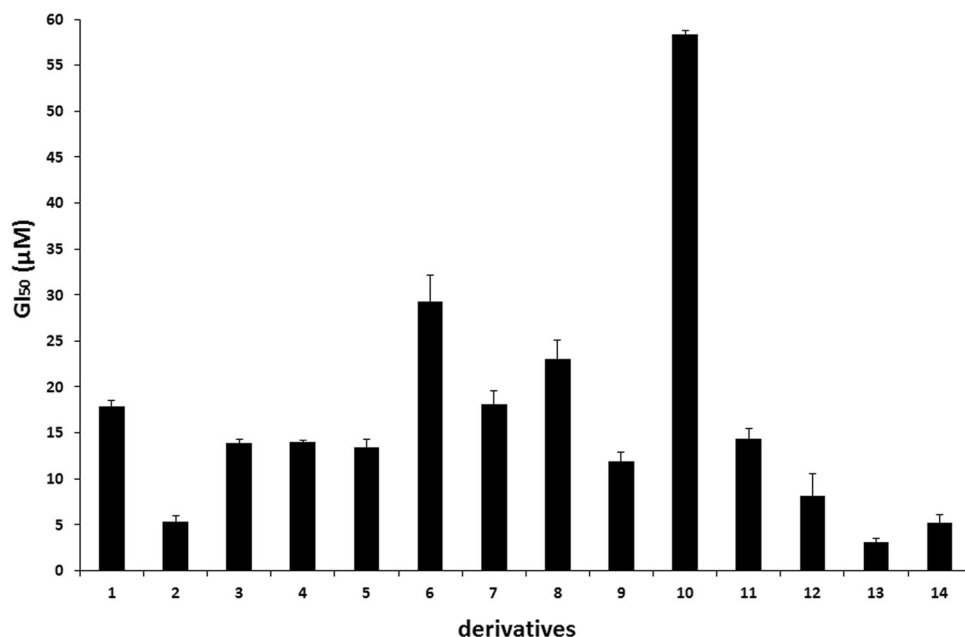
### In silico docking

For in silico docking experiments, a three-dimensional (3D) structure of derivative **13** was obtained from the crystal structure of a ligand for 1ttv.pdb and modified [31]. From the 3D structures of MDM2 deposited in the PDB, 4ode.pdb was selected for this experiment because it has



**Fig. 1** The clonogenic long-term survival assays of cells treated with 14 diphenyl imidazolines at different concentrations (0, 1, 5, 10, and 20  $\mu\text{M}$ )

**Fig. 2** The half-maximal cell growth inhibitory concentration ( $GI_{50}$ ) values in the HCT 116 human colorectal cancer cell lines of 14 diphenyl imidazolines with error bars



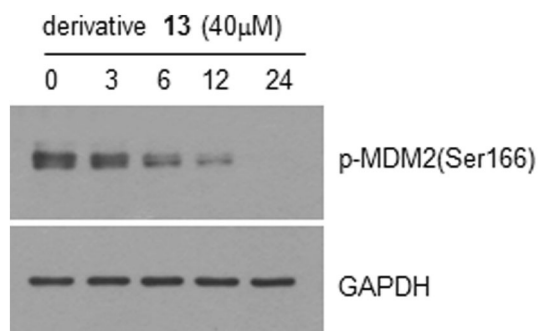
the longest chain of the N-terminal p53 interaction domain (6–110 residues) at a high resolution (1.8 Å) [32]. In silico docking experiments were performed on an Intel Core 2 Quad Q6600 (2.4 GHz) Linux PC with Sybyl 7.3 software (Tripos) [33], and LigPlot software was used to identify the binding sites [34]. All 3D images were generated using the PyMOL software (The PyMOL Molecular Graphics System, Version 1.0r1, Schrödinger, LLC).

## Results and discussion

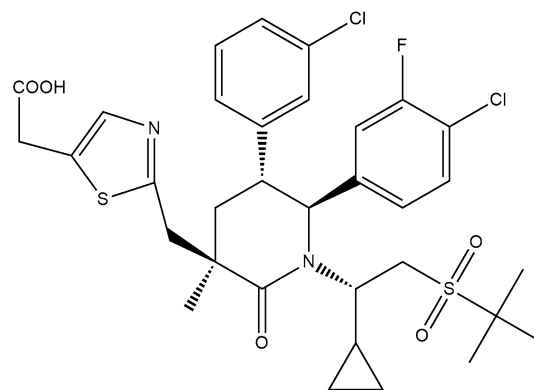
The cytotoxicities of the diphenyl imidazolines were measured using a clonogenic long-term survival assay, as shown in Fig. 1. The  $GI_{50}$  values were in the range

3.1–58.4  $\mu\text{M}$ , as listed in Table 1, and the bar graph (including errors) is shown in Fig. 2.

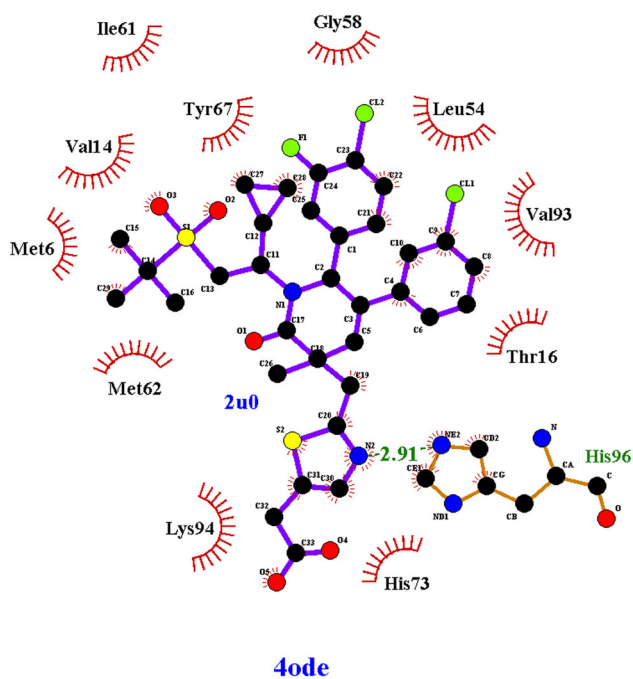
Derivatives 12 and 13 both contained a 2-naphthalenyl group, but the former was 2-naphthalen-1-yl and the latter was 2-naphthalen-2-yl. The  $GI_{50}$  values of 8.1  $\mu\text{M}$  and 3.1  $\mu\text{M}$ , respectively, indicated that the 2-naphthalen-1-yl group was a better pharmacophore than the 2-naphthalen-2-yl group was. Derivatives 5, 7, and 8 contained the halogens bromine, chlorine, and fluorine at the para position of the 2-phenyl group, respectively, with  $GI_{50}$  values of 13.4  $\mu\text{M}$ , 18.1  $\mu\text{M}$ , and 23.0  $\mu\text{M}$ , respectively. Consequently, it was shown that the electronegativity affected the cytotoxicity. Derivative 1, with a *p*-methoxy phenyl group, showed a higher  $GI_{50}$  value than did derivative 4 that contained *p*-toluene. A comparison of the derivatives 1, 2,



**Fig. 3** Effect of derivative 13 on the phosphorylation of MDM2 at S166. HCT 116 cells were treated with 40  $\mu\text{M}$  derivative 13 for different time periods. Whole cell lysates were separated by 10% SDS-PAGE, and the phosphorylation status of MDM2 on S166 was determined by immunoblotting. GAPDH was used as an internal control

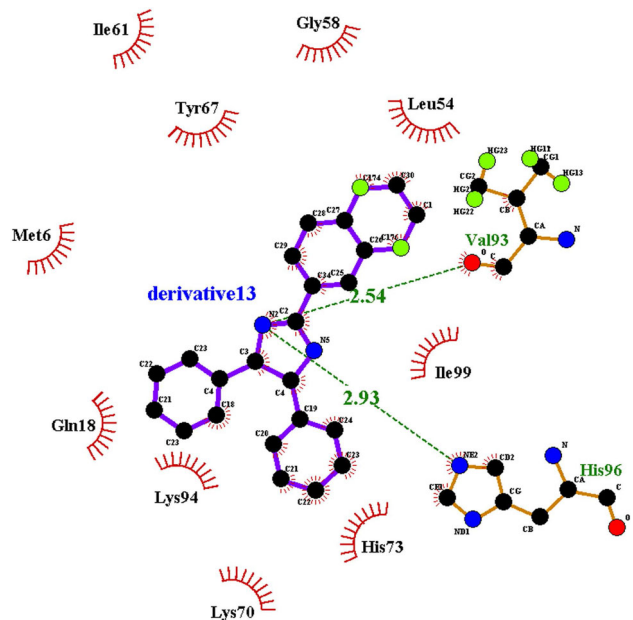


**Fig. 4** The ligand contained in the MDM2 protein (4ode.pdb), 2-[(3R,5R,6S)-1-[(1S)-2-(tert-butylsulfonyl)-1-cyclopropylethyl]-6-(4-chloro-3-fluorophenyl)-5-(3-chlorophenyl)-3-methyl-2-oxopiperidin-3-yl]methyl]-1,3-thiazol-5-yl) acetic acid



**Fig. 5** The residues participating in the binding sites of the original ligand-MDM2 complex were analyzed using the LigPlot program

and **11** revealed that the cytotoxicity was improved by an increase in the number of the methoxy groups of diphenyl imidazolines. This phenomenon agreed with the behavior of derivatives **12** and **14**. Derivative **14**, with a 4-methoxy-naphthalenyl group, showed a lower  $GI_{50}$  than did derivative **12** without the 4-methoxy group. The  $GI_{50}$  value



**Fig. 6** The residues participating in the binding sites of the derivative **13**-MDM2 complex were analyzed using the LigPlot program. The residues in half circles form hydrophobic interactions with the ligand

of derivative **9**, 2-((4R,5R)-4,5-diphenyl-imidazolin-2-yl)pyridine, was better than that of derivative **10**, 3-((4R,5R)-4,5-diphenyl-imidazolin-2-yl)pyridine, which indicated that the 2-pyridinyl group was a better pharmacophore than the 3-pyridinyl group was. This phenomenon might be caused by the different distances between the nitrogen of pyridine and the nitrogens of imidazoline. Derivative **6**, with a thiopen-3-yl group, and derivative **10**, with a pyridin-3-yl group, showed less cytotoxicity than did derivative **9**, with a pyridin-2-yl group. The distance between the two nitrogens of the former compound was 4.5 Å and that of the latter was 3.0 Å.

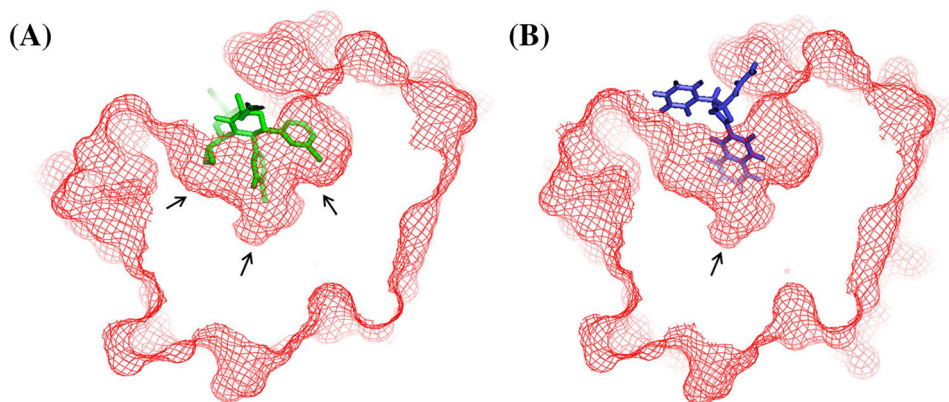
The p53 protein functions as a tumor-suppressor gene, which plays a critical role in the induction of cell cycle arrest, DNA repair, and apoptosis after diverse DNA damage responses [35–37]. MDM2 is an oncoprotein that prevents apoptosis by inducing the degradation of p53 [38]. MDM2 is activated by the phosphorylation of S166, which is mediated by the MEK/ERK or PI3 K/AKT pathways [39, 40]. As mentioned above, the anticancer effects of diphenyl imidazolines were attributable to their inhibitory effects against MDM2 [17–20]. To investigate whether the phosphorylation of MDM2 at S166 was affected by diphenyl imidazoline derivative **13** showing the most potent cell growth inhibitory effect, HCT 116 cells were subjected to treatment with 40 μM derivative **13** for different periods of time. The results indicated that the phosphorylation of MDM2 at S166 was decreased in a time-dependent manner (Fig. 3). Thus, derivative **13** efficiently inhibited the phosphorylation of MDM2 on S166.

In order to understand the binding mode of derivative **13**, which showed the strongest cytotoxicity among the derivatives tested, an in silico docking experiment was carried out. Based on the LigPlot analysis of 4ode.pdb, the ligand (short name: 2U0), (2-[[[(3R,5R,6S)-1-[(1S)-2-(tert-butylsulfonyl)-1-cyclopropylethyl]-6-(4-chloro-3-fluorophenyl)-5-(3-chlorophenyl)-3-methyl-2-oxopiperidin-3-yl]methyl]-1,3-thiazol-5-yl] acetic acid (Fig. 4), was secured by 11 hydrophobic interactions (M6, V14, T16, L54, G58, I61, M62, Y67, H73, V93, and K94) and one H-bond (H-96) (Fig. 5).

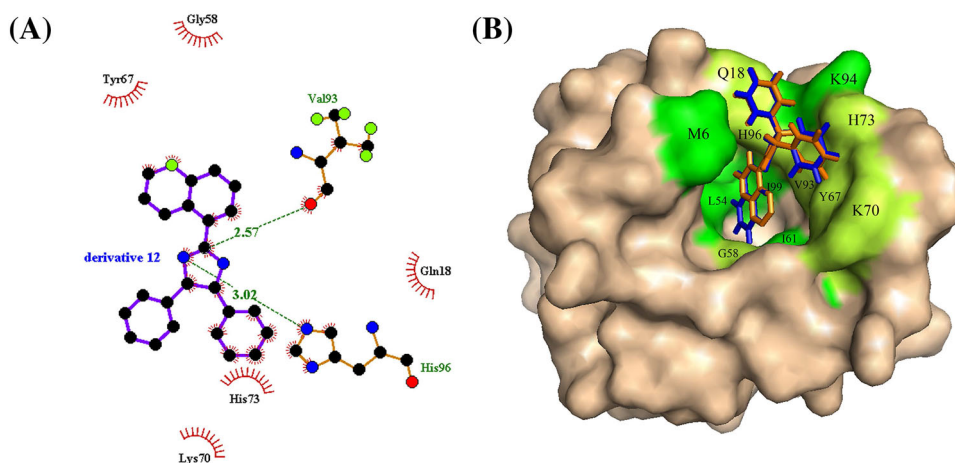
The 12 residues in the binding pocket were used for the docking experiment of derivative **13**. After docking the derivative **13** into MDM2, 30 complexes were generated from 30 docking iteration processes. The binding energy of the 30 complexes was in the range –17.80 to –10.69 kcal/mol. Among the 30 complexes, the seventh complex, with –12.14 kcal/mol of binding energy, was selected to clarify the binding mode based on both the binding pose and the binding energy. This complex was analyzed using the LigPlot program. Twelve residues were involved in the binding of derivative **13** with MDM2: M6,



**Fig. 7** The slice view of binding pocket of MDM2 complex with (A) 2U0 and (B) derivative 13



**Fig. 8** (A) The residues participating in the binding sites of the derivative 12-MDM2 complex were analyzed using the LigPlot program, and (B) shows the binding modes of derivatives 12 (orange) and 13 (blue) with MDM2. The residues colored light green interacted with derivative 12 and all 12 residues interacted with derivative 13



Q18, L54, G58, I61, K70, Y67, H73, V93, K94, H96, and I99 (Fig. 6). Two residues, V93 and H96, formed H-bonds with the nitrogen of derivative 13 and the other 10 residues showed hydrophobic interactions with the derivative. Nine residues (M6, L54, G58, I61, Y67, H73, V93, K94, and H96) were observed in both binding pockets of the original ligand of 4ode.pdb, 2U0, and derivative 13. The inside of the binding pocket was split into three small pockets. In the crystal structure of 4ode.pdb, the ligand was a good fit into these pockets (Fig. 7A) as the cyclopropyl, 4-chloro-3-fluorophenyl, and 3-chlorophenyl groups of the ligand were positioned into each of the smaller pockets. The naphthalenyl ring of derivative 13 bound to one of the pockets (Fig. 7B), which provided an explanation of the increased inhibitory activity of derivative 13 (3.1  $\mu\text{M}$ ) compared with derivative 12 (8.1  $\mu\text{M}$ ). The LigPlot analysis of the derivative 12-MDM2 complex is shown in Fig. 8A. Unlike derivative 13, derivative 12 interacts with seven residues of the protein. The binding pocket for the naphthalenyl ring, which is narrow and deep, is suitable for derivative 13, which contains 2-naphthalen-2-yl. Four residues (L54, G58, I61, and I99) bound the 2-naphthalen-2-yl group of derivative 13 (blue) via hydrophobic interactions, as shown in Fig. 8B. In contrast, it is too narrow to bind with

derivative 12 (orange), which contains 2-naphthalen-1-yl. A hydrophobic interaction was observed between MDM2 and the 2-naphthalen-1-yl group of derivative 12.

As previously mentioned, derivative 2, with tri-methoxy groups at the 2-phenyl ring, showed better inhibition compared with the activities of derivatives 1–11. This suggested that the bulky group at C-2 of imidazoline was necessary for docking into the binding pocket of MDM2.

In conclusion, we synthesized 14 diphenyl imidazoline derivatives and examined their cytotoxicities. Although the diphenyl imidazoline derivatives used in this study have only small structural differences, the  $\text{GI}_{50}$  values of the 14 derivatives in HCT 116 cells varied from 3.1 to 58.4  $\mu\text{M}$ . Based on the results of SARs and in silico docking studies, we therefore proposed that bulky groups, such as naphthalene or a highly methoxylated phenyl ring, were favored at the C-2 position of imidazoline. Additionally, branched structures were suitable for tight binding because of the presence of three small pockets.

**Acknowledgments** This work was supported by the Priority Research Centers Program [NRF, 2009-0093824]. SY Shin was supported by the KU Research Professor Program of Konkuk University.



## References

- Ueno M, Imaizumi K, Sugita T, Takata I, Takeshita M (1995) Effect of a novel anti-rheumatic drug, TA-383, on type II collagen-induced arthritis. *Int J Immunopharmacol* 17(7):597–603
- Sugita T, Ueno M, Furukawa O, Murakami T, Takata I, Tosa T (1993) Effect of a novel anti-rheumatic drug, TA-383, on type II collagen-induced arthritis—suppressive effect of TA-383 on interleukin 6 production. *Int J Immunopharmacol* 15(4):515–519
- Li YF, Gong ZH, Cao JB, Wang HL, Luo ZP, Li J (2003) Antidepressant-like effect of agmatine and its possible mechanism. *Eur J Pharmacol* 469(1–3):81–88
- Rodriguez F, Rozas I, Kaiser M, Brun R, Nguyen B, Wilson WD, Garcia RN, Dardonville C (2008) New bis(2-aminoimidazoline) and bisguanidine DNA minor groove binders with potent in vivo antitrypanosomal and antiplasmodial activity. *J Med Chem* 51(4):909–923
- Browne N, Hackenberg F, Streciwilk W, Tacke M, Kavanagh K (2014) Assessment of in vivo antimicrobial activity of the carbene silver(I) acetate derivative SBC3 using *Galleria mellonella* larvae. *Biometals* 27(4):745–752
- Ueno M, Sugita T, Murakami T, Takata I (1997) The novel anti-rheumatic drug TA-383 has a macrophage migration enhancing activity. *Jpn J Pharmacol* 74(2):221–224
- Shukla S, Bhalla M, Misra U, Mukerjee D, Saxena AK, Sinha JN, Shanker K (1998) Cardiovascular effects of novel imidazoline congeners. *Boll Chim Farm* 137(7):229–232
- Dardonville C, Goya P, Rozas I, Alsasua A, Martin MI, Borrego MJ (2000) New aromatic iminoimidazolidine derivatives as alpha1-adrenoceptor antagonists: a novel synthetic approach and pharmacological activity. *Bioorg Med Chem* 8(7):1567–1577
- Marson CM, Matthews CJ, Atkinson SJ, Lamadema N, Thomas NS (2015) Potent and selective inhibitors of histone deacetylase-3 containing chiral oxazoline capping groups and a N-(2-aminophenyl)-benzamide binding unit. *J Med Chem* 58(17):6803–6818
- Koga K, Honda K, Ando S, Harasawa I, Kamiya HO, Takano Y (2004) Intrathecal clonidine inhibits mechanical allodynia via activation of the spinal muscarinic M1 receptor in streptozotocin-induced diabetic mice. *Eur J Pharmacol* 505(1–3):75–82
- Cheng YF, Hu YZ, He QJ (2005) Synthesis and antitumor activity of arylsubstituted imidazolin-2-one derivatives. *Yao Xue Xue Bao* 40(8):711–716
- American Cancer Society. [www.cancer.org](http://www.cancer.org)
- Mosmann T (1983) Rapid colorimetric assay for cellular growth and survival: application to proliferation and cytotoxicity assays. *J Immunol Methods* 65(1–2):55–63
- Cory AH, Owen TC, Barltrop JA, Cory JG (1991) Use of an aqueous soluble tetrazolium/formazan assay for cell growth assays in culture. *Cancer Commun* 3(7):207–212
- Berridge MV, Tan AS (1993) Characterization of the cellular reduction of 3-(4,5-dimethylthiazol-2-yl)-2,5-diphenyltetrazolium bromide (MTT): subcellular localization, substrate dependence, and involvement of mitochondrial electron transport in MTT reduction. *Arch Biochem Biophys* 303(2):474–482
- Franken NA, Rodermond HM, Stap J, Haveman J, van Bree C (2006) Clonogenic assay of cells in vitro. *Nat Protoc* 1(5):2315–2319
- Zhang Z, Chu XJ, Liu JJ, Ding Q, Zhang J, Bartkovitz D, Jiang N, Karnachi P, So SS, Tovar C, Filipovic ZM, Higgins B, Glenn K, Packman K, Vassilev L, Graves B (2014) Discovery of potent and orally active p53-MDM2 inhibitors RO5353 and RO2468 for potential clinical development. *ACS Med Chem Lett* 5(2):124–127
- Carry JC, Garcia-Echeverria C (2013) Inhibitors of the p53/hdm2 protein-protein interaction-path to the clinic. *Bioorg Med Chem Lett* 23(9):2480–2485
- Ghosh P, Zhang J, Shi ZZ, Li K (2013) Synthesis and evaluation of an imidazole derivative-fluorescein conjugate. *Bioorg Med Chem* 21(8):2418–2425
- Zhang Z, Ding Q, Liu JJ, Zhang J, Jiang N, Chu XJ, Bartkovitz D, Luk KC, Janson C, Tovar C, Filipovic ZM, Higgins B, Glenn K, Packman K, Vassilev LT, Graves B (2014) Discovery of potent and selective spiroindolinone MDM2 inhibitor, RO8994, for cancer therapy. *Bioorg Med Chem* 22(15):4001–4009
- Dauwe C, Buddrus J (1995) Synthesis of enantiopure C-2-chiral amidines. *Synthesis-Stuttgart* 2:171–172
- Ishihara M, Togo H (2006) An efficient preparation of 2-imidazolines and imidazoles from aldehydes with molecular iodine and (diacetoxyiodo)benzene. *Synlett* 2:227–230
- Fujioka H, Murai K, Ohba Y, Hiramatsu A, Kita Y (2005) A mild and efficient one-pot synthesis of 2-dihydroimidazoles from aldehydes. *Tetrahedron Lett* 46(13):2197–2199
- Yong Y, Ahn S, Hwang D, Yoon H, Jo G, Kim YH, Kim SH, Koh D, Lim Y (2013) 1H and 13C NMR spectral assignments of 2'-hydroxychalcones. *Magn Reson Chem* 51(6):364–370
- Ahn S, Shin SY, Jung Y, Jung H, Kim BS, Koh D, Lim Y (2016) (1) H and (13) C NMR spectral assignments of novel flavonoids bearing benzothiazepine. *Magn Reson Chem* 54(5):382–390
- Shin SY, Jung H, Ahn S, Hwang D, Yoon H, Hyun J, Yong Y, Cho HJ, Koh D, Lee YH, Lim Y (2014) Polyphenols bearing cinnamaldehyde scaffold showing cell growth inhibitory effects on the cisplatin-resistant A2780/Cis ovarian cancer cells. *Bioorg Med Chem* 22(6):1809–1820
- Yoon H, Kim TW, Shin SY, Park MJ, Yong Y, Kim DW, Islam T, Lee YH, Jung KY, Lim Y (2013) Design, synthesis and inhibitory activities of naringenin derivatives on human colon cancer cells. *Bioorg Med Chem Lett* 23(1):232–238
- Jung Y, Shin SY, Yong Y, Jung H, Ahn S, Lee YH, Lim Y (2015) Plant-derived flavones as inhibitors of aurora B kinase and their quantitative structure-activity relationships. *Chem Biol Drug Des* 85(5):574–585
- Shin SY, Ahn S, Yoon H, Jung H, Jung Y, Koh D, Lee YH, Lim Y (2016) Colorectal anticancer activities of polymethoxylated 3-naphthyl-5-phenylpyrazoline-carbothioamides. *Bioorg Med Chem Lett* 26(17):4301–4309
- Jung H, Shin SY, Jung Y, Tran TA, Lee HO, Jung KY, Koh D, Cho SK, Lim Y (2015) Quantitative relationships between the cytotoxicity of flavonoids on the human breast cancer stem-like cells MCF7-SC and their structural properties. *Chem Biol Drug Des* 86(4):496–508
- Fry DC, Emerson SD, Palme S, Vu BT, Liu CM, Podlaski F (2004) NMR structure of a complex between MDM2 and a small molecule inhibitor. *J Biomol NMR* 30(2):163–173
- Gonzalez AZ, Li Z, Beck HP, Canon J, Chen A, Chow D, Duquette J, Eksterowicz J, Fox BM, Fu J, Huang X, Houze J, Jin L, Li Y, Ling Y, Lo MC, Long AM, McGee LR, McIntosh J, Oliner JD, Osgood T, Rew Y, Saiki AY, Shaffer P, Wortman S, Yakowec P, Yan X, Ye Q, Yu D, Zhao X, Zhou J, Olson SH, Sun D, Medina JC (2014) Novel inhibitors of the MDM2-p53 interaction featuring hydrogen bond acceptors as carboxylic acid isosteres. *J Med Chem* 57(7):2963–2988
- Shin SY, Yoon H, Hwang D, Ahn S, Kim DW, Koh D, Lee YH, Lim Y (2013) Benzochalcones bearing pyrazoline moieties show anti-colorectal cancer activities and selective inhibitory effects on aurora kinases. *Bioorg Med Chem* 21(22):7018–7024
- Wallace AC, Laskowski RA, Thornton JM (1995) LIGPLOT: a program to generate schematic diagrams of protein-ligand interactions. *Protein Eng* 8(2):127–134

35. Fridman JS, Lowe SW (2003) Control of apoptosis by p53. *Oncogene* 22(56):9030–9040
36. Yin Y, Tainsky MA, Bischoff FZ, Strong LC, Wahl GM (1992) Wild-type p53 restores cell cycle control and inhibits gene amplification in cells with mutant p53 alleles. *Cell* 70(6):937–948
37. Zhan Q (2005) Gadd45a, a p53- and BRCA1-regulated stress protein, in cellular response to DNA damage. *Mutat Res* 569(1–2):133–143
38. Kubbutat MH, Jones SN, Vousden KH (1997) Regulation of p53 stability by Mdm2. *Nature* 387(6630):299–303
39. Malmlof M, Roudier E, Hogberg J, Stenius U (2007) MEK-ERK-mediated phosphorylation of Mdm2 at Ser-166 in hepatocytes. Mdm2 is activated in response to inhibited Akt signaling. *J Biol Chem* 282(4):2288–2296
40. Zhou BP, Liao Y, Xia W, Zou Y, Spohn B, Hung MC (2001) HER-2/neu induces p53 ubiquitination via Akt-mediated MDM2 phosphorylation. *Nat Cell Biol* 3(11):973–982